Indian Journal of Pure & Applied Physics
Vol. 61, January 2023, pp. 33-42
DOI: 10.56042/ijpap.v61i1.67262

Mechanical Testing of Hybrid LM30 Metal Matrix Composite Fabricated through Stir Casting Route

Vivek Joshi[a], Leeladhar Nagdeve[a], Girija Moona[b,c] & Harish Kumar[a]*

[a]Department of Mechanical Engineering, National Institute of Technology, Delhi, 110 040, India

[b]CSIR National Physical Laboratory, New Delhi, 110 012, India

[c]Academy of Scientific and Innovative Research, Ghaziabad, 201 002, India

Received 9 October 2022; accepted 18 November 2022

Metal Matrix Composites (MMCs) are one of the strongest contenders for the application that demands excellent mechanical and physical properties. Aluminium Metal Matrix Composites (Al MMCs) are reinforced materials with improved mechanical and physical properties as compared to the base material. Composite material made through the stir casting process possesses higher elastic modulus, wear resistance, strength, and fatigue resistance. In the present research work, LM30 alloy is chosen as a matrix material and is reinforced with Zircon Dioxide (ZrO_2), Rice Husk Ash (RHA), and Tungsten Carbide (W.C.). A stir casting setup is used to fabricate the three different composites. Composite A, Composite B, and Composite C have the composition of (LM30/5%WC/5%ZrO_2/10%RSH), (LM30/10%WC/5%ZrO_2/5RSH), (LM30/5%WC/10%ZrO_2-/5% RHA), respectively. Further, mechanical testing, which includes tensile, compressive, hardness, and Charpy impact tests, has been conducted. It has been found that Composite B possesses the highest hardness, maximum tensile, and compressive strength among all three composite materials.

Keywords: Stir casting; LN30 Metal matrix composite; Tensile test; Compressive test; Hardness; Charpy test

1 Introduction

When two or more constituents that differ in form and chemical nature and are insoluble in each other are combined macroscopically, so that achieved properties are significantly different from the constituents, the material obtained is called composite. Matrix is a continuous phase that supports reinforcement while reinforcement is added to enhance the physical and mechanical properties such as wear behaviour, friction coefficient, and thermal conductivity. The stir casting process is a widely used manufacturing process because of its simplicity, flexibility, and low production cost. AMMCs are used for various automotive, aerospace, and biomedical applications. Numerous metals have been identified as matrices. The most critical MMC systems are the Aluminium matrix, Magnesium matrix, Titanium matrix, Copper matrix, Super alloy matrices, *etc*. Metal matrix composite is produced with standard techniques, such as extrusion, forging or rolling, *etc*. The reinforced materials are mixed into the matrix in a definite route to change the strength of composites.

Figure 1 shows the stir casting setup mainly composed of a stirring assembly and a furnace.

During the production of MMCs, various parameters need to be considered. Thangarasu *et al*.[1] studied the measured content of TiC powders reinforced with MMC, compacted into a groove of 0.5mm × 5.5mm. They found that 45% increased hardness of the composite material by friction stirring process than the matrix alloy. Asuquo *et al.*[2] found that the mechanical properties (hardness, tensile stress, and percentage elongation) of the casting from

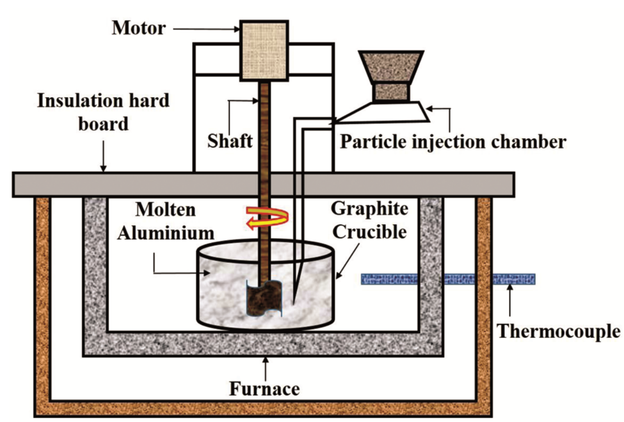

Fig. 1 — Stir Casting Process.

*Corresponding author:
(E-mail: harishkumar@nitdelhi.ac.in)

imported zircon sand (167.55BHN, 509.55N/mm2, 8%) are better than those from the local zircon sand (159.17BHN, 347.13N/mm2, and 0.15%). Composite with LM-13 as matrix and silicon dioxide particulates as reinforcement were fabricated by varying the percentage of silicon dioxide particulates in the steps of 3 from3 to 12% by Rao *et al.*[3]. It was found that with an increase in silicon dioxide, the strength of composite material increased and became maximum at nine wt% of silicon; after that, it decreased. Henein *et al.*[4] and Zachary *et al.*[5] reported that TiC reinforcement brings enhancement in hardness and wear resistance; however, it was observed that this enhancement was higher for small particle (0.6-3.5μm) reinforcement as compared to relatively large particle (0.8-5.6μm) reinforcement. Viswanathan *et al.*[6] reported the remelting of the 2124A-10wt%SiC composite at 800 °C and 900 °C resulted in the composite interface and reduced volume of SiC particles from top to bottom of the remelted composite plate. Bobic *et al.*[7] reported that SiC brings higher wear resistance and lower friction coefficient in A356 aluminium alloy composite than Al_2O_3 particles, which can be attributed to the favorable arrangement of SiC particles. Das *et al.*[8] fabricated the Aluminium alloy Silicon Carbide based composite material for automobile brake drum application and found improved results than cast iron.

Authors reported the variation of damping characteristics of aluminium matrix by varying the percentage of graphite (Gr) particulates as reinforcement[9]. Olivier *et al.*[10] Concluded that addition of Mg catalyzes the Al_4C_3 formation while adding (Zn + Mg) and Cu improved the strength of composites. Gul *et al.*[11] fabricated the composite Al–10Si/SiCp via vacuum infiltration. When subjected to the sliding wear test, wear rate reduces with increasing the weight percentage of SiC particles while wear increases with increased applied load. Huber *et al.*[12] investigated the thermal expansion characteristics of different AMMC/SiC composites by subjecting them to a temperature up to 5000 °C. Visco-plastic matrix deformations were used to investigate the coefficient of thermal expansion. Investigation of dry sliding characteristics of Al-Si-SiCp composite revealed that composite containing equal size reinforcement have lower friction coefficient and wear compared to a composite containing reinforcement in a wide range of size Uyyuru *et al.*[13]. Ahlatci *et al.*[14] fabricated the composite by reinforcing the Al with 25 vol.% SiC particles, 37 vol.% Al_2O_3 and Mg up to 8%. It was noticed that as compressive Strength and hardness increase, toughness and porosity decrease. With Mg addition, the wear resistance of composite increases. Gu *et al.*[15] reported the damping behavior and Mechanical properties of SiO_2f/ /Al_2O_3/ SiCp/Mg hybrid composite fabricated by the liquid pressure infiltration technique. It was observed that the damping characteristics were enhanced significantly by Mg addition. Kang *et al.*[16] investigated the Al+SiC+Gr and Al+SiC composite, which showed that a composite containing only SiC as reinforcement possessed uniform distribution of particles compared to a composite containing SiC and Gr. SiC particles as reinforcement improved the fatigue characteristics, bending strength, and hardness Kaynak *et al.*[17]. SiC enhanced the fatigue strength by acting as hurdles to cracks. Singh *et al.*[18] studied the comparative investigation of corrosion characteristics of cast iron, LM13-10% SiCp, and Al-Cu-based LM-13 alloy composite. It was observed that compared to composite, base alloy possessed better corrosion characteristics, whereas poor corrosion resistance was seen in cast iron. Gandhi *et al.*[19] found that when in the solid-liquid mixture, solid particle size varies over a wide range of mass, and average particle size should be used instead of average particle size. Composites having different contents of tubular halloysite nanotubes (HNTs) and low-density polyethylene (LDPE) were investigated by Polanskýa *et al.*[20]. HNTs inhibited heat release due to the burning of LDPE. HNTs basically toughened the LDPE matrix. Das *et al.*[21] fabricated the composite material by choosing two different matrix alloys, such as Al-Si alloys (LM30 of hypereutectic and LM13 of near eutectic composition) by casting method. It was found that there was approximately 50% reduction in the friction coefficient of the LM30 and LMl3 composite when graphite particle dispersion. Singh *et al.*[22] analyzed the two-body abrasive wear characteristics of LM30/SiC composite and studied various properties associated with mechanical, microstructure, and physical aspects. Compared to matrix alloy, an increment of 30% in the yield strength, 17% in ultimate tensile strength and 38% in hardness of the composite was found. However, 48% reduction in elongation of the composite was observed. Zamani *et al.*[23] found 35% and 44% rise in total elongation and ultimate tensile strength, respectively in hot extruded aluminium-matrix composite that was subjected to high-temperature annealing. It was observed that the distribution of SiCp has a significant impact, due to which the melt flow got retarded Rajak *et al.*[24]. Akbar

Table 1 — Chemical Composition of Al-Si Alloy (LM30 alloy)

LM30 alloy	Si	Fe	Cu	Mn	Mg	Zn	Ti	Ni	Pb	Sn	Al
Wt%	11.8	0.3	1.2	0.4	0.9	0.2	0.02	0.9	0.02	0.005	Balance

et al.[28] compared oil and water quenching, Brine quenching results in higher hardness and distortion. A higher cooling rate generates thermal stress that initiates the crack. Shekhar *et al.*[25] analyzed the mechanism of strains and stresses, surface generation, thermal softening, de-bonding, particle fracture, chip formation, wear modes, and dislocation phenomena, in the turning process. Sharma *et al.*[26] studied the impact of heat treatment on the dry sliding wear properties of sillimanite reinforced LM30 composites fabricated via Stir casting. Composites subjected to T6 heat treatment exhibited superior hardness as compared to T4 heat treated and normal composites. Also, compared to other composites, the friction coefficient of T6 heat-treated composites was quite lower. Sathish *et al.*[27] used LM30 as a matrix and reinforced it with graphite (6%), Silicon Carbide (4%), and boron carbide (2%). It was found that 4% silicon carbide as reinforcement results in higher enhancement in impact strength.

A lot of experimental work has been reported to analyze the wear behavior of the stir-casted or sintered aluminium alloy matrix composite. The reinforcement influences the wear rate and wear behaviour together with other mechanical properties. Various reinforcement have been found to increase the wear resistance of the composite. For hybrid composite, the corrosion resistance does not depend upon the type of reinforcement. The protective coating over the Al-based hybrid composite's surface curbs the wear rate. For tungsten carbide and Zirconia reinforced aluminium alloy cast samples, an increase in W.C. and $ZrSiO_4$ resulted in a rise in the wear resistance and hardness with a decrease in the ductility. Further, research works need to be carried out on hybrid aluminium matrix composite by varying the weight percentage of reinforcement such as silicon carbide, Zirconia, and tungsten carbide to find out the different mechanical properties, wear behaviour, microstructure and hardness of tungsten carbide and Zirconia as hybrid composite need to be studied.

2 Materials and Methods

2.1 Synthesis of LM30/ZrO2/SiC/ RHA Hybrid Composite

The essential characteristics of Aluminium are lightweight, good electrical conductivity, high corrosion resistance, good machinability, and easy availability. The main drawback is its low hardness and poor strength. Addition of alloying elements like silicon, copper, manganese, and magnesium can increase its strength up to four times. Strength of Aluminium alloy can be increased further by heat treatment (age hardening); due to increased strength, aluminium alloys are extensively used in commercial applications. The major drawback of aluminium casting is higher solidification shrinkage. For nomenclature, the aluminium association uses a three-digit numerical system. At the same time, British standards have the prefix L.M. Aluminium silicon alloys are preferred because of the high fluidity, which is attributed to the presence of a large amount of the Al-Si eutectic. The eutectic is formed at 12.6%. Slow solidification of the Al-Si alloy results in the formation of coarse microstructure. In contrast, the eutectic solution of Al-Si alloy consists of a needle and large plates of silicon in a continuous aluminium matrix. Al-Si alloy (LM30 alloy) was chosen as the matrix material, whose composition is shown below in Table 1.

Table 2 — Percentage of reinforcement used in the composite

Composite	Reinforcement (wt%)		
	WC	ZrO_2	RUSH
A	5	5	10
B	10	5	5
C	5	10	5

Tungsten carbide, Silicon carbide, and Zirconia was used as reinforcement material with Particle size in the range of 20-53 µm shown in Table 2. The stir casting setup is composed of a stirrer assembly and a resistance furnace. The stirrer, which had three blades separated by an angle of 120° was fabricated by shaping and cutting the graphite block. This stirrer was linked with a variable velocity (0 to 1700 rpm) motor via a steel shaft. Inside the machine's furnace, a crucible that had the capacity to take 1.5kg Al melt was placed. Around 700 gms of LM30 alloy was remelted under 820 °C in the furnace. Under 450 °C, Preheating of zircon sand, rice husk ash, and silicon carbide mixture was carried out in a resistance furnace in order to eliminate the various gases and moisture from the reinforcement. The stirrer was then allowed to move vertically downward (nearly around 3 cm measured from the bottom of the crucible). After that, stirrer, velocity was gradually increased to

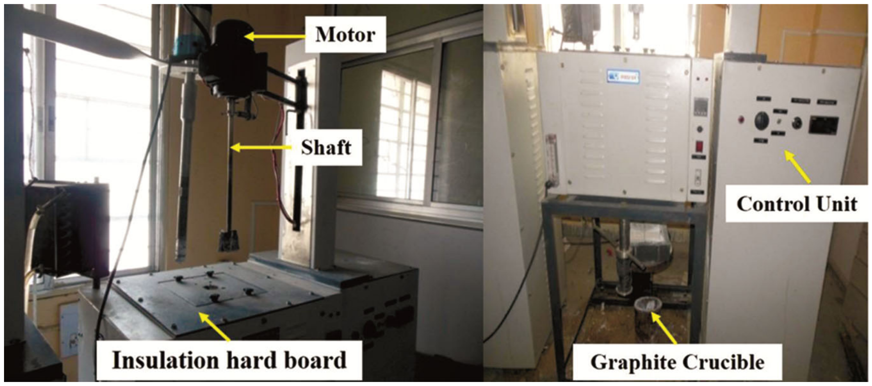

Fig. 2 — Photographic view of Stir Casting setup.

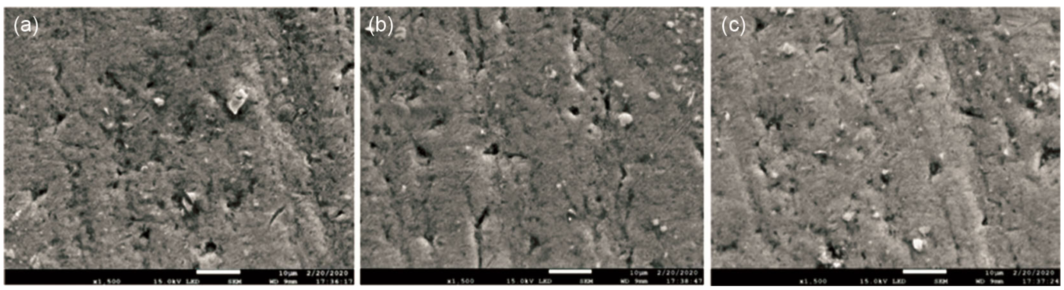

Fig. 3 — SEM Image of fabricated composites.

700 rpm, and the preheated mixture of reinforcements, Zirconia, Silicon carbide, and RHA, was added using ladle a spoon at a rate of 10- 20g/min. During stirring, as the melt solidifies, its viscosity increases which tend to reduce stirrer speed, so a speed control mechanism is attached to the stirrer, which helps to maintain the desired speed. After stirring, the melt was allowed to come to rest and kept in the static condition for 1 min. Finally, the melt was poured into two small metal moulds (dia 1.5 cm × length 10 cm) and (3cm× 3cm×11cm) successively. Fig. 2 shows the photographic view of the experimental setup.

Scanning electron microscopy (SEM) was used to investigate the surface characteristics of the composite, while EDS was done to know the elemental distribution of the composite.

The density of the particles is a crucial property that plays an important role during the fabrication of the composite. The reinforcements that have a density lower than the density of melt tend to segregate at the top, while reinforcement having a higher density than the melt tends to settle at the bottom. Since the properties of the composite are quite dependent upon reinforcement distribution, hence the uniform distribution of reinforcement particles is quite desirable. Several investigators reported that fracture occurs in the matrix in ductile mode. The microstructure of the specimen had analyzed as per the procedure given in the ASM standard. The sample had etched with killer reagent solution. SEM analysis is also done from a specific area of the sample, and a 2-D image is generated. Fig. 3 shows the SEM.

The properties of reinforcement such as Zirconia, Tungsten carbide, and RHA are listed in Table 3, Table 4, and Table 5, respectively.

Table 3 — Properties of Zirconia

Properties	Zirconium Dioxide (ZrO_2)
M.P.(°C)	2500
Limit of application (°C)	1870
Hardness(Moh's Scale)	7.5
Density(g/cm^3)	5.68
Linear coefficient Of expansion(10^{-6K})	4.5
Fracture toughness(MPa-m)	5
Crystal structure	Monoclinic

Table 4 — Properties of Tungsten Carbide

Properties	Tungsten Carbide (W.C.)
M.P. (°c)	2870
Limit of application (°c)	1800
Linear coefficient of expansion (10^{-6k})	5.5
Density g/cm^3	15.63
Hardness (Moh's scale)	9-9.5
Fracture toughness(MPa-m$^{1/2}$)	7.34
Crystal structure	Hexagonal

2.2 Brinell Hardness Test

Hardness is a property of a material by virtue of which it offers resistance to indentation. For hardness testing, a fixed load of magnitude 150N was applied for 10sec via a 5 mm diameter hardened steel ball. Brinell hardness number was determined on the basis of the surface area of the indentation and applied load. To maintain the perpendicularity of the surface of the specimen and to obtain a regular indentation shape on the specimen, it was polished before hardness testing.

The test result obtained nine mass loss values corresponding to three average durometer hardness values obtained for the normal 50, 60, and 70 durometer rubber wheels. Normalize the mass loss values to correspond to the travel of the wheel having dia 177.8 mm and a width of 12.7 mm using the formula. Normalized mass loss values and volume loss are calculated using Equation 1 and Equation 2, respectively.

Table 5 — Properties of RHA.

Properties	Rice Husk Ash (RHA)
M.P. (°c)	1440
Limit of application (°c)	700
Density g/cm^3	0.15

$$Normalized\ mass\ loss\ values\ in\ gm = \frac{177.8 \times 12.7 \times actual\ mass\ lossingms}{actual\ dia\ in\ mm \times actual\ width\ in\ mm} \quad \ldots (1)$$

$$Volume\ loss\ in\ mm^3 = \frac{mass\ loss\ in\ gms \times 1000}{density\ (gms/cm3)} \quad \ldots (2)$$

3 Results and Discussion

3.1 Microstructure Analysis

Tungsten Carbide (W.C.), Zirconium dioxide (ZrO_2), and RHA particles of size 20-50 μm were used as reinforcement in LM30 alloy. Figs. 4, 5, and 6 depicts the EDS analysis of composite materials.

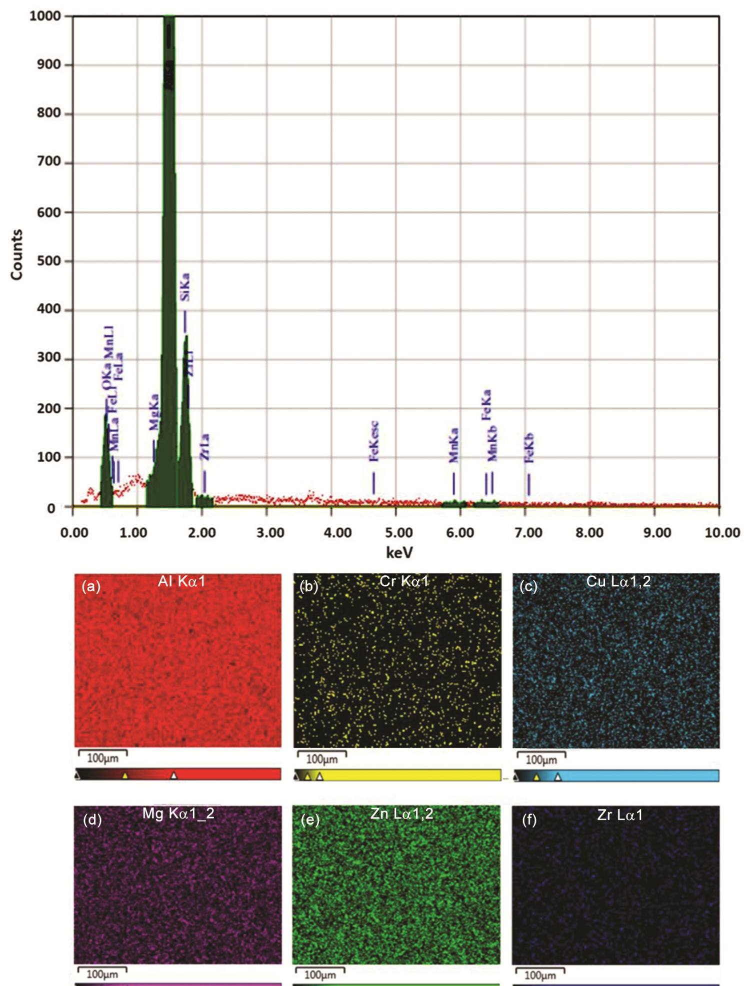

Fig. 4 — EDS Image of Composite A.

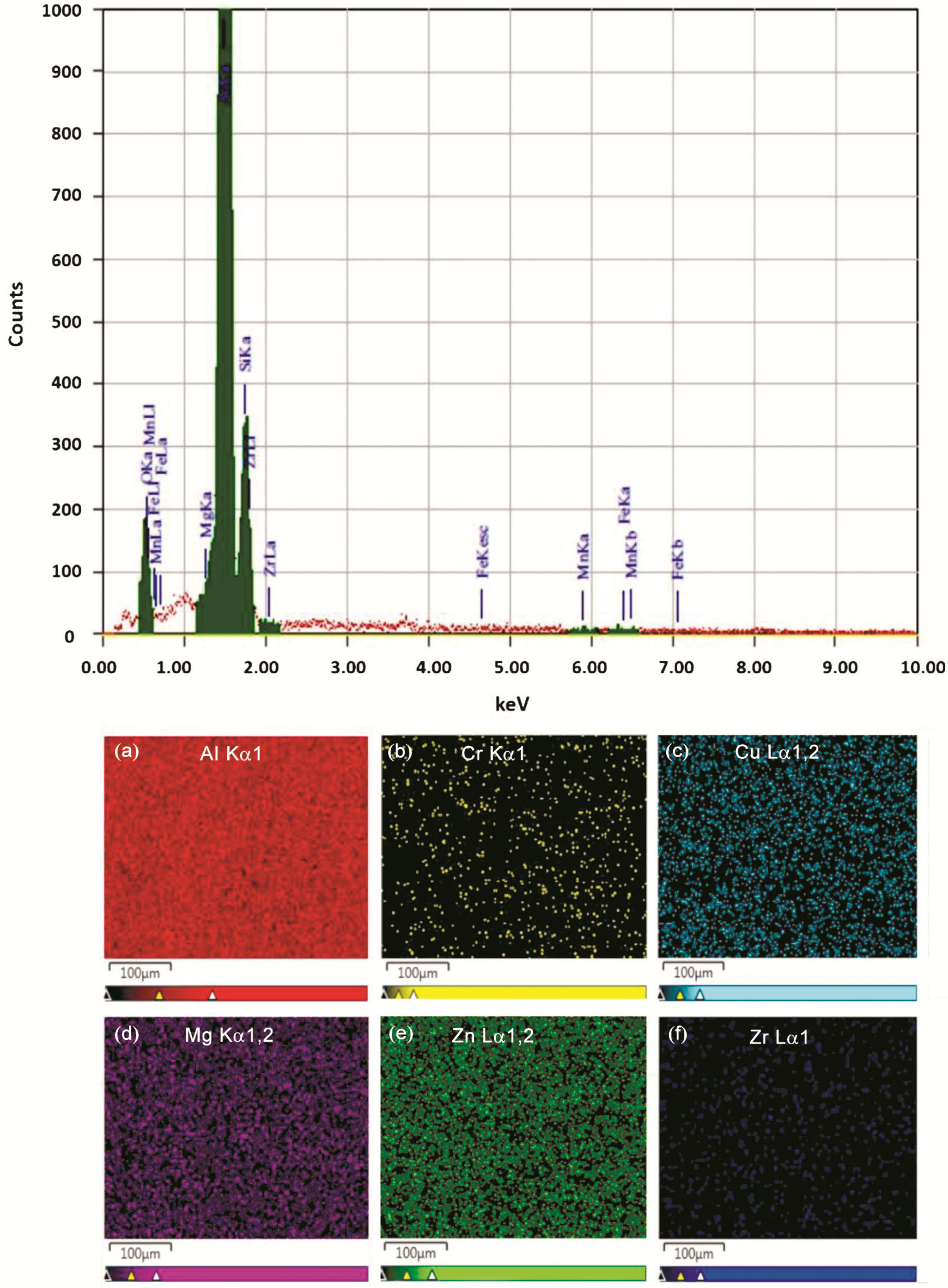

Fig. 5 — (a-g) EDS Image of Composite B.

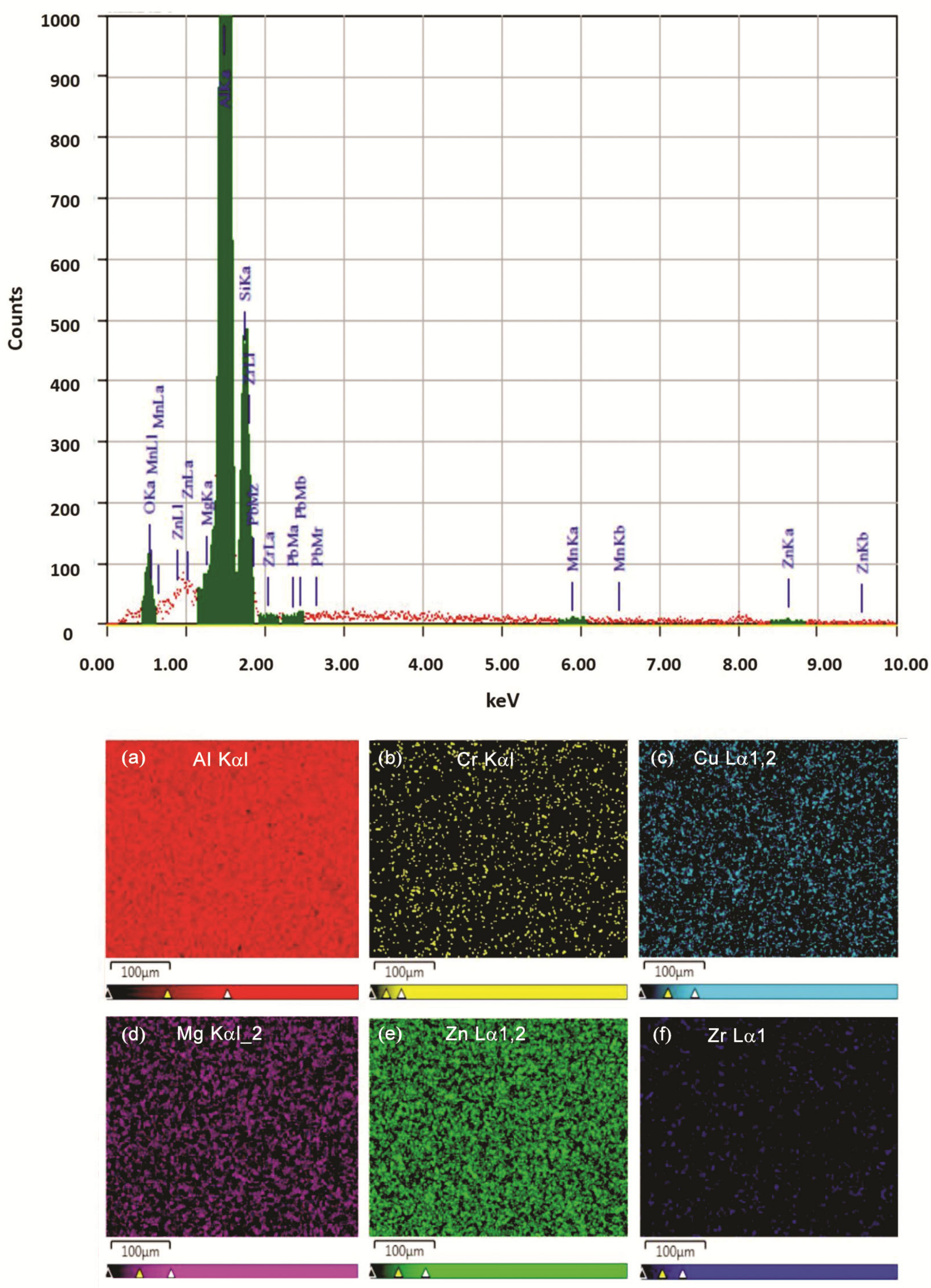

Fig. 6 — (a-g) EDS Image of Composite C.

3.2 Mechanical Testing

Table 6 represents the hardness and density of the fabricated composites material

3.3 Compressive Test

A compressive test was performed at room temperature. Fig. 7 depicts the photographic view of the sample before and after the compressive test.

Table 7 shows the compressive strength of the composite material fabricated through the stir casting process.

The compressive test shows that composite B possessed the highest compressive strength compared to that of composites C and A, which can be attributed to the presence of maximum tungsten carbide *i.e.*, 10% in composite B (Fig. 8).

Table 6 — Hardness and Density

COMPOSITE	A	B	C
HARDNESS (BHN)	94	91	87
DENSITY (g/cm^3)	2.725	2.742	2.757

Table 7 — Compressive strength of fabricated composites materials

COMPOSITE	A	B	C
Ultimate compressive load (K.N.)	24.000	38.520	20.080
Ultimate compressive Strength (N/mm^2)	305.577	490.451	255.66
Deflection at ultimate load (mm)	2.800	4.700	2.200
Maximum deflection (mm)	3.200	4.900	3.900

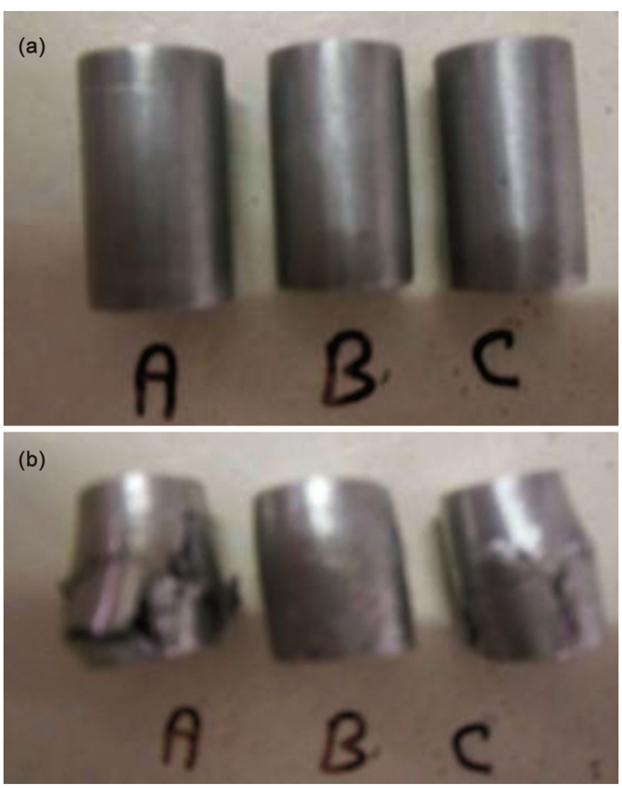

Fig. 7 — (a) Specimen Before test; (b) after compressive test.

3.4 Tensile Test

The following Fig. 9 shows the test specimen before and after the tensile test. Again composite B has high tensile load than composite A and C in a tensile test. The yield strength in tension, ultimate tensile strength, and breaking tensile stress is maximum for composite B (Fig. 10).

3.5 Charpy Impact Test

The Charpy test is basically a strain rate test that is used to find the energy absorbed by the specimen just before fracture.

Table 8 shows the data related to the Charpy test for all the composites. The Charpy test showed that composite B has the highest energy absorption capacity compared to composite A and C (Fig. 11). It can be predicted that composite B has a higher value of tungsten carbide.

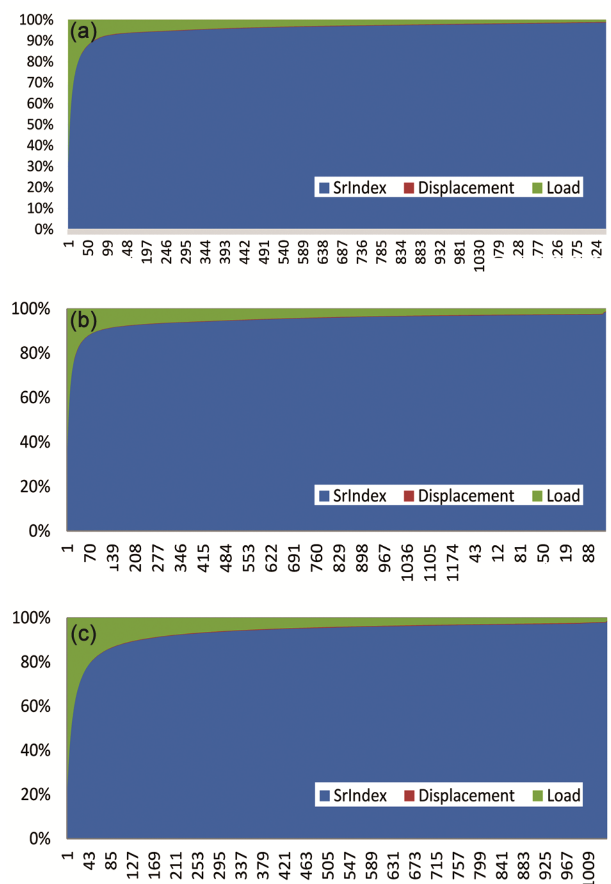

Fig. 8 — Compressive Strength of Composite A, B, and C.

Table 8 — Charpy Impact test of the manufactured composites materials

Composite	Size (l x b x t) mm	Depth of Notch (mm)	Rupture (or Impact) energy (kg-m)	Modulus of Rupture (kg/m^2)	Notch Impact Strength (kg/m)
A	55 x 10 x 10	2	1.5	$3.4x\ 10^5$	$1.86x\ 10^4$
B	55 x 10 x 10	2	1.8	$4.09x10^5$	$2.25x\ 10^4$
C	55 x 10 x 10	2	1.6	$3.6x\ 10^5$	$2x\ 10^4$

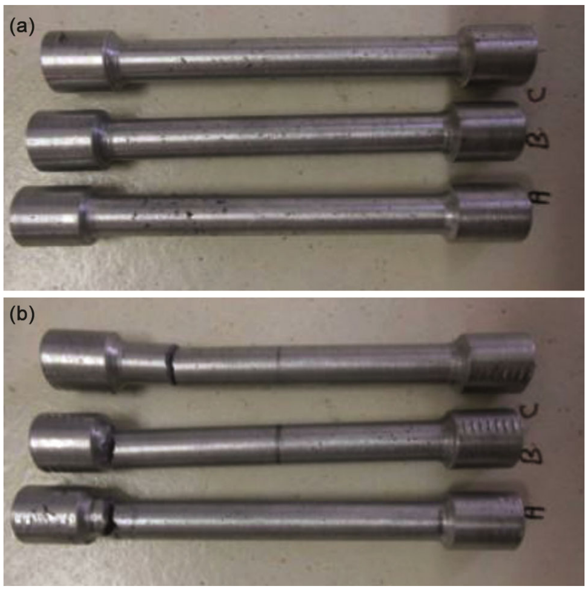

Fig. 9 — Tensile test of Composites: (a) Before; (b) After.

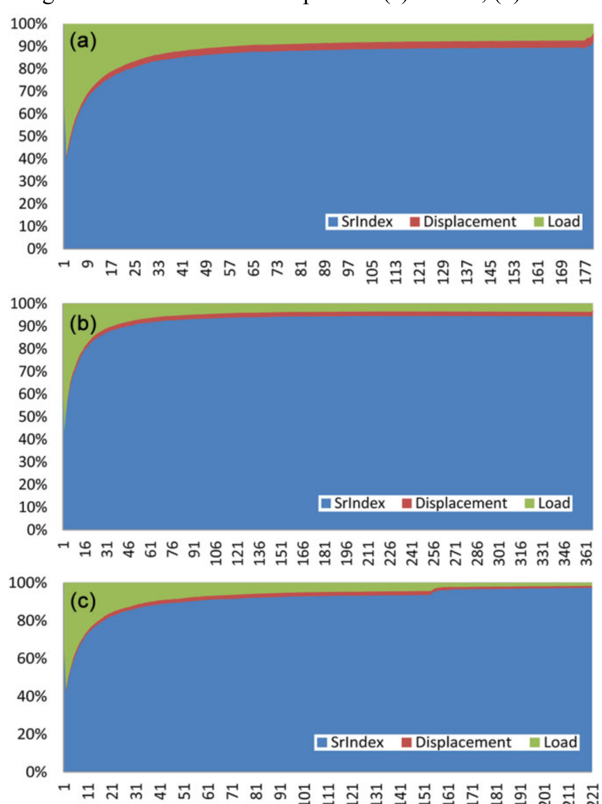

Fig. 10 — Tensile Strength of Composite A, B, and C.

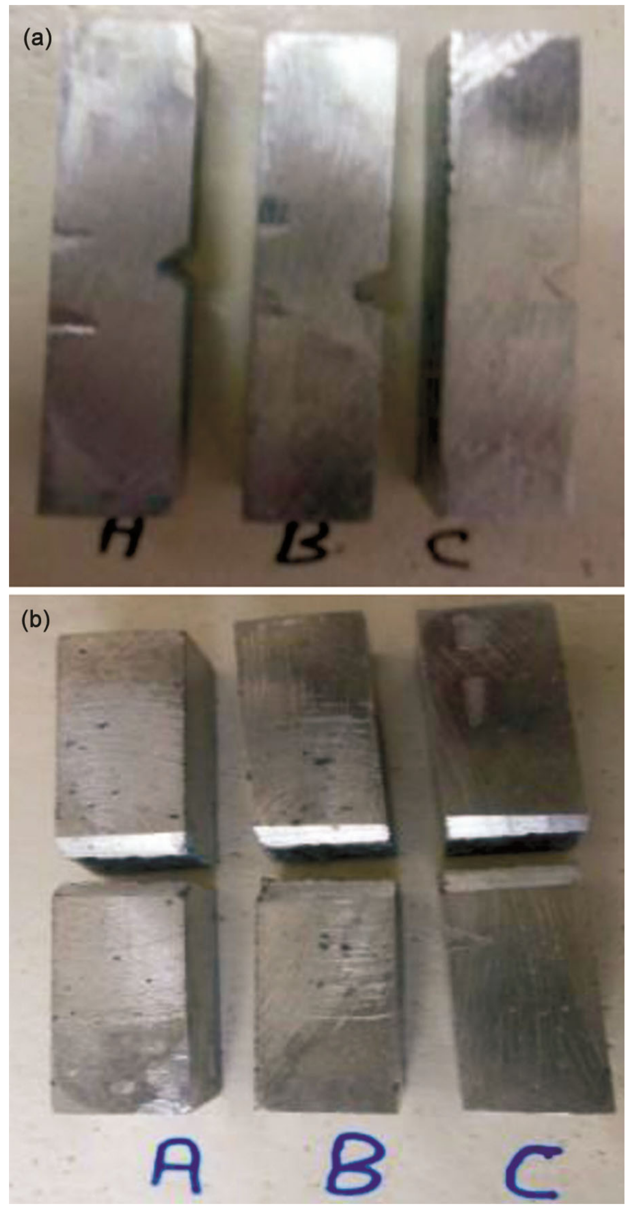

Fig. 11 — Specimen of composites: (a) Before impact test; and (b) After impact test.

4 Conclusions

The present work was done to know the relative effect of hybrid reinforcement on microstructure, and mechanical properties of stir-casted LM30 alloy composites. From the comparative investigation of three composites, namely A, B, and C, we can draw the following conclusion:

- Since the RSH carries out the grain refinement, which ultimately leads to the increase in hardness; hence the composite A (LM30/5%WC/5%ZrO_2/10%RHA), which consists of the highest amount of RSH compared to another composite, possessed the maximum hardness compared to composite B (LM30/10%WC/5%ZrO_2/10%RHA) and composite C (LM30/5%WC/10%ZrO_2/10%RSH).
- Since W.C. promotes good internal bonding, therefore, the composite B (LM30/10% WC/5%ZrO_2/10%RHA), which has the higher W.C. content, has the highest mechanical properties (tensile strength, compressive strength, impact strength) compared to composite A (LM30/5%WC/5%ZrO_2/10%RHA) and composite C (LM30/5%WC/10%ZrO_2-/10%RHA).
- It was seen that the higher the rpm, the deeper would be the plowing marks which can be attributed to the fact that at higher rpm, the rupturing of mechanically mixed layer gets accelerated.

Declaration of Conflict of Interest

The authors whose names are listed as authors certify that they have NO affiliations with or involvement in any organization or entity with any financial interest (such as honoraria; educational grants; participation in speakers' bureaus; membership, employment, consultancies, stock ownership, or other equity interest; and expert testimony or patent-licensing arrangements), or non-financial interest (such as personal or professional relationships, affiliations, knowledge or beliefs) in the subject matter or materials discussed in this manuscript.

Date Access Statement

All data that support the findings of this study are included within the article (and any supplementary files).

Acknowledgment

This work was supported by the National Institute of Technology Delhi, India (Ministry of Education, Government of India).

Ethics Statement

The research project has been conducted ethically, keeping in mind privacy, consent and appropriate reporting of those involved in the study.

References

1 Thangarasu A, Murugan N, Dinahara I & Vijay S J, *Indian Acad Sci*, 37 (2012) 579.
2 Asuquo L O, Bassey E N & Ihoms A P, *J Mech Indus Res*, 1 (2013) 27.
3 Mallikarjuna G B, Rao K V S & Jaypraksh R H, *Int J Mech Eng Robot Res*, 1 (2012).
4 Katelyn H, Unlu N, Goller G, Öveçoğlua M L & Henein H, *Comp Part A: Appl Sci Manuf*, 42 (2011) 812.
5 Zachary A & Mohsen O S, *Ceram Int J*, 38 (2012) 4263.
6 Mandal D & Viswanathan S, *Mater Character*, 86, (2013) 21.
7 Vencl A, Bobic I, Arostegue S, Bobic B, Marinkovic A & Babic M, *J Alloys Compd,* 506 (2010) 631.
8 Rehman, Das S & Dixit D, *Tribol Int J*, 51 (2012) 36.
9 Wei J N, Cheng H F, Zhang Y F, Han F S, Zhou Z C & Shui J P, *Mater Sci Eng*, 325 (2002) 444.
10 Before O, Long S, Cayron C, Kuebler J & Buffat P A, *Comp Sci Technol,* 67 (2007) 737.
11 Gu F & Aguilar M, *Comp Sci Technol*, 64 (2004) 1959.
12 Huber T, Degischer H P, Lefranc G & Schmitt T, *Comp Sci Technol*, 66 (2006) 2206.
13 Uyyuru R K, Surappa M K & Brusethaug S, *Tribol Int J,* 40 (2007) 365.
14 Ahlatci H, Kocer T, Candan E & Huseyin C, *Tribol Int J*, 39 (2016) 213.
15 Gu J, Zhang X, Gu M, Gu M & Wang X, *J Alloys Compd*, 372 (2004) 304.
16 Gui M & Kang S B, *Mater Lett*, 51 (2001) 396.
17 Kaynak C & Boyle S, *Mater Des*, 27 (2006) 776.
18 Singh I B, Singh M, Das S & Gupta A K, *Indian J Chem Technol,* 19 (2012) 385.
19 Gandhi B K, Borse S V, *Wear,* 257 (2004) 73.
20 Polanský R, Kadlec P, Slepička P, Kolská Z & Švorčík V, *Polym Testing,* 78 (2019) 105993,
21 Das S & Prasad S V, *Wear,* 33 (1989) 173.
22 Singh R K, Telang A & Das S, *Trans Nonferrous Met Soc*, 30 (2020) 65.
23 Zamani R, Mirzadeh H & Emmy M, *Mater Sci Eng A,* 726 (2018) 10.
24 Rajak D K, Kumaraswamidhas L A, Das S, Kumaran S S, *J Alloys Compd*, 656 (2016) 218.
25 Sekhar R & Singh T P, *J Mater Res Technol*, 4 (2015) 197.
26 Sharma S, Nanda T & Pandey O P, *Wear,* 426 (2019) 27.
27 Sathish T, Saravanan S & Vijayan V, *Mater Res Innovat*, 24 (2020).
28 Akbar H I, Surojo E, Ariawan D & Prabowo A R, *Res Eng,* 6 (2020).